Diffusion-Weighted Imaging with Sensitivity Encoding (SENSE) for Detecting Cranial Bone Marrow Metastases: Comparison with T1-Weighted Images

Won-Jin Moon, MD[1,2]
Min Hee Lee, MD[1]
Eun Chul Chung, MD[1]

Objective: This study was designed to determine whether diffusion-weighted imaging (DWI) with sensitivity encoding (SENSE) could detect bone marrow involvement in patients with cranial bone marrow (CBM) metastases. DWI results obtained were compared with T1-weighted imaging (T1WI) findings.

Materials and Methods: DWI with sensitivity encoding (SENSE; b value = 1,000) was performed consecutively in 13 patients with CBM metastases diagnosed pathologically and radiologically. CBM lesions were dichotomized according to the involved site, i.e., skull base or calvarium. Two radiologists qualitatively evaluated the relative conspicuousness of CBM lesions and image qualities in B0 and in isotropic DWI and in T1WI. According to region of interest analysis of normal and pathologic marrow for these three sequences, absolute signal difference percentages (SD%) were calculated to quantitatively analyze lesion contrast.

Results: All 20 lesions in 13 patients with CBM metastases revealed abnormal DWI signals in areas corresponding to T1WI abnormalities. Both skull base and calvarial lesions provided better lesion conspicuousness than T1WI and B0 images. Although the image quality of DWI was less satisfactory than that of T1WI, relatively good image qualities were obtained. Quantitatively, B0 images (SD%, 82.1 ±7.9%) showed better lesion contrast than isotropic DWI (SD%, 71.4 ±13.7%) and T1WI (SD%, 65.7 ±9.3%) images.

Conclusion: For scan times of less than 30 seconds, DWI with SENSE was able to detect bone marrow involvement, and was superior to T1WI in terms of lesion conspicuity. DWI with SENSE may be helpful for the detection of cranial bone/bone marrow metastases when used in conjunction with conventional MR sequences.

Index terms:
Brain, MR
Bone marrow, MR
Magnetic resonance (MR), comparative studies
Magnetic resonance (MR), diffusion-weighted imaging

Korean J Radiol 2007;8:185-191
Received November 14, 2006; accepted after revision February 27, 2007.

[1]Department of Radiology, Kangbuk Samsung Hospital, Sungkyunkwan University School of Medicine, Seoul 110-746, Korea; [2]Department of Radiology, Konkuk University Hospital, Konkuk University School of Medicine, Seoul 143-701, Korea

This research was supported by a grant from Kangbuk Samsung Hospital, Korea.

Address reprint requests to:
Eun Chul Chung, MD, Department of Radiology, Kangbuk Samsung Hospital, Sungkyunkwan University School of Medicine, 108 Pyung-dong, Chongno-gu, Seoul 110-746, Korea.
Tel. (822) 2001-1031
Fax. (822) 2001-1030
e-mail: ec.chung@samsung.com

CBM = cranial bone marrow
CHESS = chemical shift selective
DWI = diffusion-weighted imaging
EPI = echo-planar imaging
FLAIR = fluid attenuation inversion recovery
PET = positron emission tomography
SD% = signal difference percentages
STIR = short-T1 inversion recovery

Magnetic resonance imaging (MRI) is regarded as the best imaging modality for assessing bone marrow because it provides high resolution and is able to clearly distinguish fat from other tissues (T1WI). Normal fatty marrow is hyperintense on T1-weighted images while normal red (active, cellular, hematopoietic) bone marrow produces a hypointense signal compared to yellow (fatty) marrow on T1WI. In the adult population, cranial bone marrow is mostly comprised of yellow fatty marrow that produces a high signal on T1WI. However, increased hematopoiesis in patients with anemia or cellular infiltration in patients with bone/bone marrow metastases can cause bone marrow to appear hypointense on T1WI (1−6). During routine brain MRI examinations, bone/bone marrow lesions in the skull base and calvarium are often encountered, but cannot always be identified as such with certainty, and often they are missed due to a complex anatomy, interpreter inexperience, or may be simply overlooked.

Recently, several investigators have examined the use of diffusion-weighted imaging (DWI) for evaluating bone marrow lesions, especially in the spine (7−14). On routine echo-planar diffusion-weighted images, normal yellow fatty marrow appears hypointense due to the fat suppression technique implemented in DWI. In addition, highly cellular areas are observed as relatively hyperintense areas by DWI. Using sensitivity encoding (SENSE), DWI provides artifact-reduced images with shorter acquisition times (14). However, no studies are currently available concerning the use of DWI for investigating cranial bone marrow.

We undertook this study to evaluate whether DWI with SENSE is able to detect bone marrow involvement in patients with cranial bone/bone marrow metastases, and to compare DWI and T1WI findings.

METHODS

Patients

The study consisted of 13 consecutive patients over a six month period (9 women and 4 men; age range, 34−73 years; median age, 61 years). These patients were referred for MR imaging of known or clinically suspected intracranial metastases. Of these 13 patients, 12 had a known primary tumor (breast cancer, n = 3; lung cancer, n = 5; stomach cancer, n = 1; rectal cancer, n = 1; lymphoma, n = 1; multiple myeloma, n = 1), and the remaining patient was diagnosed with an unknown primary tumor. In 10 patients, cranial bone/bone marrow metastases were diagnosed based on conventional radiography and/or CT findings, and by initial and follow-up bone scintigraphy in addition to MR imaging. For two patients, diagnosis was confirmed using a pathologic specimen. In one patient who did not undergo initial CT or bone scintigraphy, diagnosis was confirmed at a three month follow-up by MR imaging and bone scintigraphy. For comparison purposes, 13 healthy age-matched volunteers (8 women and 5 men; age range, 33−73 years; median age, 61 years) were examined by using the same MR protocol.

Written informed consent was obtained from all patients prior to imaging, and the study was approved by our institutional review board.

MR Imaging

All images were acquired using a six-channel SENSE head coil on a 1.5-T MR scanner (Intera; Philips Medical Systems, Best, the Netherlands). The routine conventional MR imaging protocol included: 1) sagittal and axial T1-weighted spin-echo (420/11 [repetition time (TR) msec/echo time (TE) msec]); 2) axial T2-weighted fast spin-echo (4000/100 [effective echo time]; 3) axial FLAIR (fluid attenuation inversion recovery (6000/120/2000 [inversion time]); and, 4) axial and coronal T1-weighted spin-echo after gadolinium contrast injection. The parameters of conventional MR imaging were; a 256 ×192 matrix, a 23-cm field of view, and a 5 mm slice thickness with a 1 mm intersection gap. Single-shot spin-echo echo-planar DWI sequences were obtained by applying six diffusion gradients in different directions for each slice, and two diffusion weightings (b values = 0 and 1,000 sec/mm^2). Isotropic DWI were generated on-line by averaging six images with different diffusion gradients. Non-diffusion-weighted B0 images were also obtained. DWI examinations involved the acquisition of 20 slices using the following parameters; 3200/66 (TR/TE), a 256 ×128 matrix, a 23 cm field of view, and a 5 mm slice thickness with a 1 mm intersection gap. The chemical shift selective (CHESS) technique was implemented for fat suppression, and apparent diffusion coefficient (ADC) maps were also obtained at a workstation (EasyVision; Philips Medical Systems, Eindhoven, The Netherlands).

Imaging Analysis

One neuroradiologist and one musculoskeletal radiologist who were unaware of the patient clinical histories reviewed all images; any disagreements were resolved by consensus. All bone/bone marrow lesions were allocated to one of two subgroups, i.e., lesions involving the calvarium and lesions involving the skull base. When a bone marrow lesion involved the clivus, petrous bone, or occipital condyle, it was defined as a skull base lesion. Multiple small lesions in one subgroup were considered to be a single lesion. The presence or absence of a bone/bone marrow lesion was determined in each set of the three different sequences. On DWI, an abnormal bone/bone marrow signal was defined as a lesion iso- or hyperintense to gray matter. A visual comparison was then made of each lesion with regard to its relative conspicuousness. Relative conspicuousness was graded using a four-point scale (1, poor; 2, moderate; 3, good; 4, excellent). Overall image quality relative to artifact severity was also rated for each sequence using a four-point scale (1, poor; 2, moderate; 3, good; 4, excellent). For qualitative analysis, we also displayed DWI on an inverted gray-white scale.

For quantitative analysis, one neuroradiologist measured the signal intensities of regions of interest (ROI) of the bone marrow lesions and of the adjacent normal marrow. ROIs ranged from 14 to 50 mm^2. In ROI in B0, isotropic DWI, and T1WI, the absolute signal difference (%) was calculated as follows: $|A-B|/(A+B)\times100$, where A is the signal intensity of pathologic marrow and B that of

normal marrow. The ADC values of ROI were also obtained (15). Contrast-to-noise ratios (CNR) (calculated using CNR = $|A-B|/\sigma$, where σ = the standard deviation of the background signal intensity), could not be obtained because background noise is systematically removed by applying SENSE.

Statistical Analysis

SPSS (Version 12; SPSS Inc., Chicago, IL) was used for the statistical analysis, and the Kruskal-Wallis test with post hoc analysis was used to compare signal difference (%) and ADC ratios between the three groups. Significance was accepted at the $p < 0.05$ level.

RESULTS

No abnormal lesions of the bone/bone marrow were observed by DWI and conventional sequences in the 13 healthy volunteers. However, a total of 20 lesions were found in the 13 patients (Table 1): nine lesions were located in the clivus and 11 in the calvarium. In all patients with cranial bone/bone marrow metastases, abnormal signal intensities were detected on DWI (B0 and isotropic image) areas corresponding to T1WI abnormalities (Fig. 1). In both the clival and calvarial regions, the relative conspicuousness of lesions by DWI tended to be better than that by T1WI. Compared with T1WI and B0 images, isotropic images showed more conspicuous lesions (Table 2). Although the image quality of DWI was less satisfactory than that of T1WI, DWI provided relatively good image quality (Table 3). Even in the clival region, the image qualities of the isotropic and B0 DWI were mainly good (n = 8, 88.9%) or excellent (n = 7, 77.8%) (Fig. 2).

On B0 images, the absolute signal difference percent between normal and pathologic bone marrow was 82.1 ± 7.9%, on isotropic DWI 71.4 ±13.7%, and on T1WI, 65.7 ±9.3% ($p < 0.001$, Kruskal-Wallis test). By post hoc paired comparisons, the absolute signal differences on B0 DWI were significantly higher than those of T1WI ($p < 0.01$), but no significant difference was found between

Table 2. Comparison of DWI and T1WI in Terms of the Relative Conspicuousness of Cranial Bone Marrow Metastasis (n = 20)

	Superior to T1WI	Equivalent to T1WI	Inferior to T1WI
iDWI	11	5	4
B0	7	7	6
iDWI + B0	12	4	4

Note.—T1WI: T1-weighted images, B0 = echo-planar T2-weighted images, iDWI = isotropic diffusion-weighted images.

Table 1. Clinico-radiological Data in Patients with Cranial Bone Marrow Metastases

Case No.	Sex	Age	Location	Diagnosis	Relative Conspicuousness			Image Quality		
					T1WI	B0	iDWI	T1WI	B0	iDWI
1	M	73	Clivus	Unknown primary	4	3	3	4	4	4
2	F	72	Calvarium	Lung cancer	4	4	4	4	4	4
3	M	69	Clivus	Lung cancer	3	3	4	4	4	4
			Calvarium		3	3	4	4	4	4
4	F	71	Calvarium	Lung cancer, small cell	2	4	3	4	4	3
5	F	67	Clivus	T cell lymphoma	3	2	2	4	3	2
6	M	64	Clivus	Stomach cancer	2	1	1	4	2	2
			Calvarium		3	1	1	4	2	2
7	F	55	Clivus	Lung cancer, small cell	3	2	4	4	4	4
			Calvarium		4	4	4	4	4	4
8	M	58	Calvarium	Lung cancer, adenoma	3	4	3	4	4	4
9	F	34	Clivus	Breast cancer	2	3	4	4	4	4
			Calvarium		3	4	4	4	4	4
10	F	44	Clivus	Breast cancer	3	4	4	4	4	4
			Calvarium		3	3	4	4	4	4
11	F	61	Clivus	Multiple myeloma	4	4	4	4	4	4
			Calvarium		4	4	4	4	4	4
12	F	44	Clivus	Breast cancer	2	3	4	4	4	4
			Calvarium		2	3	3	4	4	4
13	F	55	Calvarium	Rectal cancer	3	2	4	4	4	4

Note.—T1WI = T1-weighted images, B0 = echo-planar T2-weighted images, iDWI = isotropic diffusion-weighted images
F = female, M = male, 1 = poor, 2 = fair, 3 = good, 4 = excellent

isotropic DWI and T1WI ($p > 0.05$). The mean ADC value of pathologic bone marrow was $0.90 \pm 0.25 \times 10^{-3}$ mm²/s ($0.48 - 1.21 \times 10^{-3}$ mm²/s). However, the ADC of normal bone marrow could not be determined due to signal nullification by the fat-suppression technique.

Table 3. Comparison of DWI and T1WI with Respect to Image Quality of Cranial Bone Marrow Metastases (n = 20)

	Superior to T1WI	Equivalent to T1WI	Inferior to T1WI
iDWI	0	16	4
B0	0	17	3
iDWI + B0	0	17	3

Note.—T1WI = T1-weighted images, B0 = echo-planar T2-weighted images, iDWI = isotropic diffusion-weighted images.

DISCUSSION

Considering both the qualitative and quantitative data obtained during this study, DWI is comparable, and in some cases, superior to T1WI at detecting cranial bone/bone marrow metastases. In particular, the B0 and isotropic DWIs were of sufficient high quality for detecting bone/bone marrow metastases in the clivus and calvarial regions.

All metastatic lesions demonstrated high signal intensity (SI) on B0 and isotropic DWIs, as compared to the SI of normal bone/bone marrow. Tumor-related hypercellularity and T2-shine-through effects may have contributed to DWI findings (9–11). Dense tumor cell packing, such as that seen in metastatic tumors, reduces extracellular volume and as a result limits water proton diffusion (9).

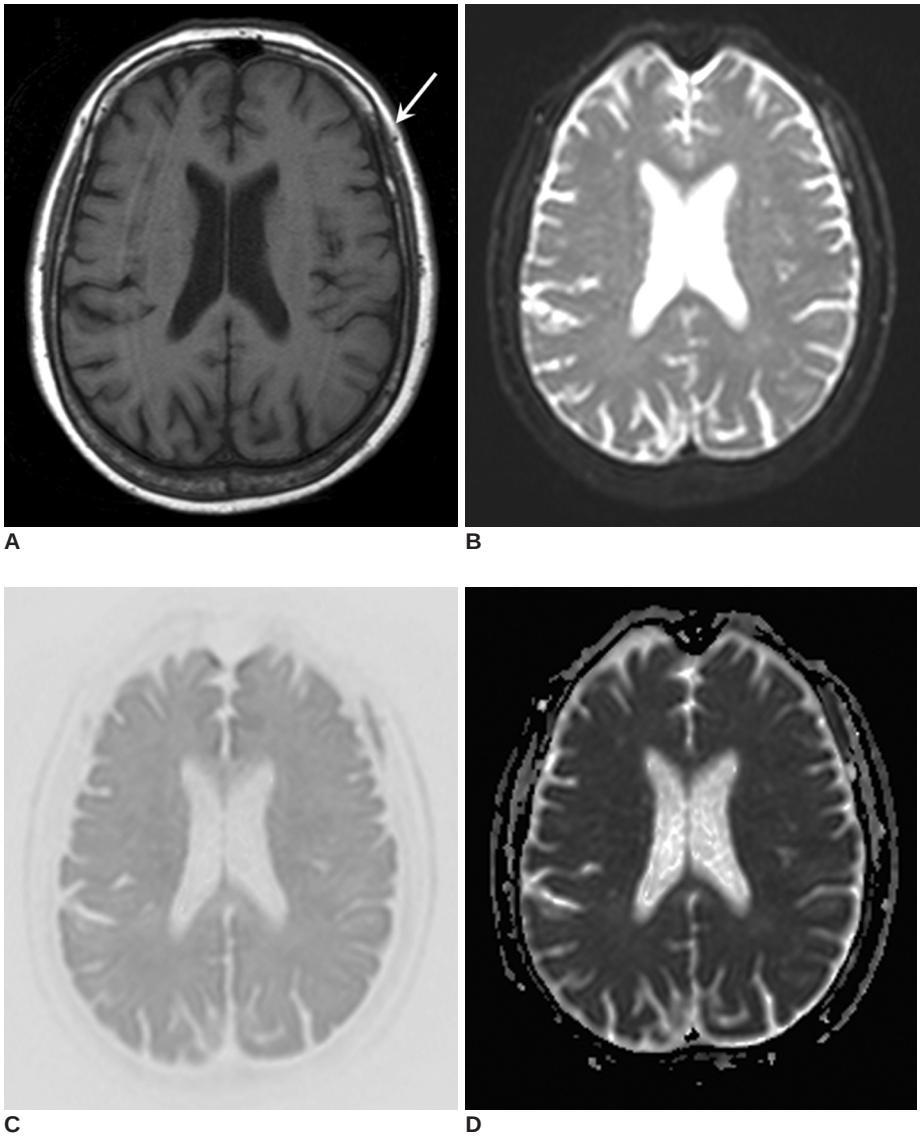

Fig. 1. A 71-year-old woman with lung cancer (case no. 4). T1-weighted image (**A**), B0 image (**B**), isotropic diffusion-weighted image (**C**), and an apparent diffusion coefficient map (**D**) were obtained. Abnormalities in signal intensity due to bone marrow metastases (arrow) are evident on all images. However, the relative lesion conspicuousness is better on the B0 image and the isotropic diffusion-weighted image than on the T1-weighted image.

Limited diffusion appears as high signal intensity on DWIs and as reduced ADC values on ADC maps. When a relatively small b value (< 250 s/mm^2) and a relatively long TE is used, the T2 shine-through effect may dominate the diffusion effect (13, 15). We used a high b value of 1,000s/mm^2 and the shortest TE available to minimize the T2 shine-through effect. In addition, the decreased ADC values of metastases observed in the present study imply that tumor hypercellularity is more important for diffusion hyperintensity than the T2 shine-through effect (11, 13).

T2-weighted imaging with some form of fat suppression, such as short-TI inversion recovery (STIR) and fat-suppressed T2-weighted imaging, is regarded as the most valuable method for detecting bone marrow lesions (16). By suppressing the fat signal from normal adult fatty bone marrow, better lesion contrast can be achieved for bone marrow abnormalities. For DWI using echo-planar imaging (EPI), the fat-suppression technique is implemented, since the EPI method is highly susceptible to resonance effects, such as the water-fat shift (11). Thus, the B0 imaging conducted during this study represents an EPI equivalent to fat-suppressed T2-weighted spin-echo sequence imaging without using diffusion gradients.

The isotropic DWIs represent averages of at least more than six diffusion gradient images, and thus show tissue diffusability in any direction. Therefore, isotropic DWI minimizes the T2-relaxation effect and maximizes diffusion sensitivity, which may be useful for detecting and grading highly cellular tumors (17). Moreover, signals from normal fatty marrow are suppressed during isotropic DWI. One

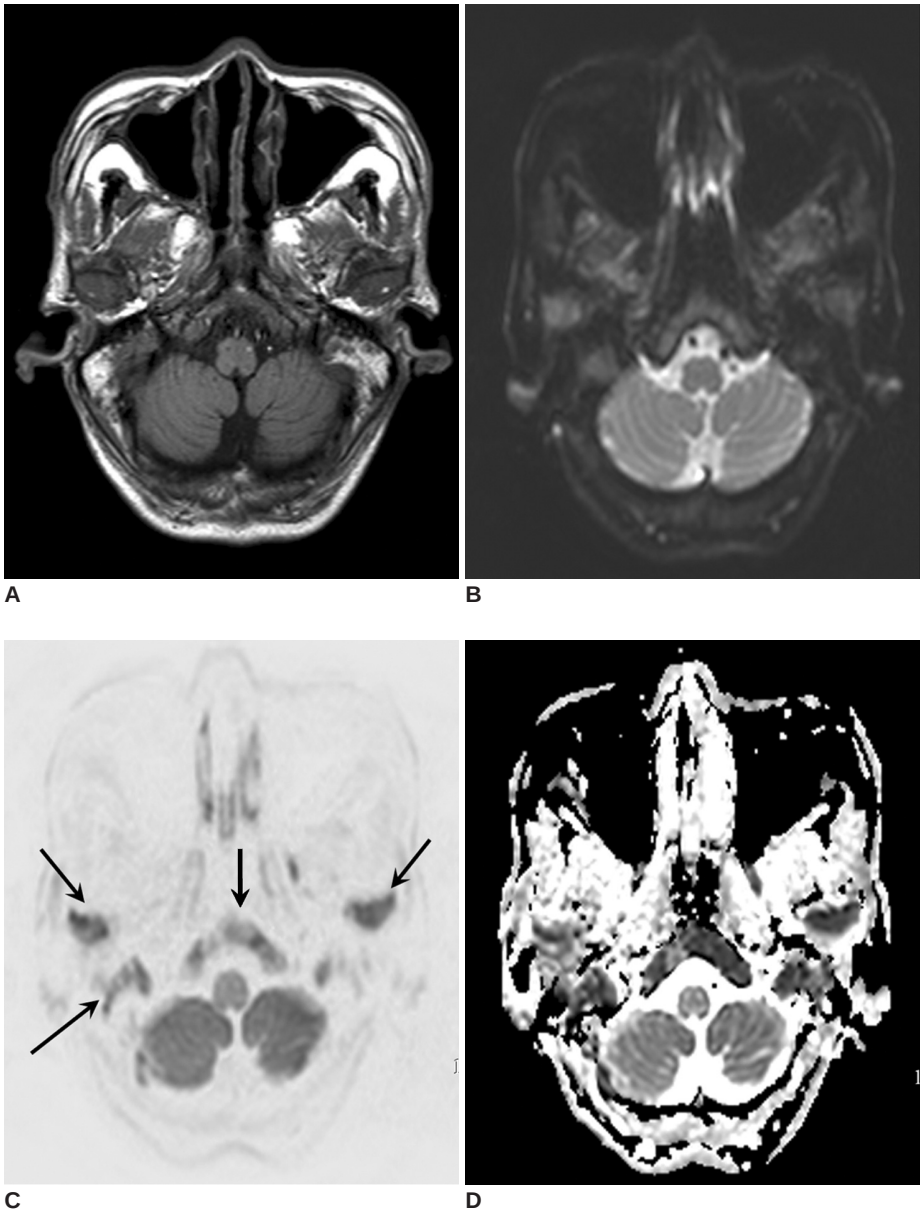

Fig. 2. A 69-year-old man with lung cancer (case no. 3). T1-weighted image (**A**), B0 image (**B**), isotropic diffusion-weighted image (**C**), and an apparent diffusion-coefficient map (**D**) were obtained. Lesions involving the skull base and mandibular condyles (arrows) are visible on all images. However, the isotropic diffusion-weighted image shows a superior lesion contrast.

could argue that a poorer signal to noise ratio (SNR) and a lower spatial resolution of isotropic diffusion images versus conventional MR sequences contraindicate its use for metastasis detection. However, we present here comparable, and sometimes better lesion contrast for isotropic DWI than T1WI. For qualitative analysis of lesion detection by DWI, we displayed DWI images in an inverted gray-white scale, i.e., as negative contrast images, which are similar to bone scintigraphy or positron emission tomography (PET) images, allowing easier comparisons with scintigraphic or PET images (18).

Although isotropic images showed superior relative conspicuousnesses when T1WI or B0 images were compared on a qualitative basis, quantitative analysis showed best lesion contrast for B0 images. This discrepancy between quantitative and qualitative analysis may have resulted from the complex background signals from different tissues on the B0 images, which tend to obscure lesions. Moreover, sampling errors associated with ROI placement, particularly in terms of signal difference percentage computations, may also have contributed to this discrepancy. Most importantly, the B0 images show everything with longer T2 relaxation as a high SI, and as a result, one cannot easily differentiate actual lesions from unimportant background signals. However, B0 images do provide better anatomical detail and soft tissue contrast than isotropic DWI alone. Therefore, we used a combination of B0 and isotropic DWI for lesion detection and felt that this improved the relative conspicuousness.

In this study, no remarkable difference in lesion conspicuousness was observed between the skull base and calvarium. The complex skull base anatomy can prevent radiologists from detecting infiltrative lesions in various MR sequences, including T1WI, and the less experienced radiologist or trainee may miss subtle abnormal signals of skull base involvement because of its complexity. DWI with the echo-planar technique is known to be problematic for evaluations of the posterior fossa and skull base, because of prominent magnetic susceptibility artifacts near air-bone interfaces (19). However, the use of a parallel imaging technique, such as SENSE, can markedly reduce magnetic susceptibility artifacts in the skull base, and when using this technique, DWI shows good lesion contrast and image quality for the detection of bone/bone marrow lesions. Moreover, reliable diffusion-weighted images can be obtained quickly (less than 30 seconds) using SENSE.

The mean ADC value of metastatic lesions in the present study was $0.90 \pm 0.25 \times 10^{-3}$ mm^2/s, which is consistent with data from previous studies in which vertebral metastases and malignant compression fractures showed ADC values that ranged from 0.69×10^{-3} to 0.92×10^{-3} mm^2/s (7, 11, 12, 20). The relatively wide range of ADC values encountered during the present study may have been due to varying degrees of necrosis within the metastases and tumor cellularity. Tumor necrosis within a metastatic lesion is known to cause an increase its ADC value (12).

There is no consensus concerning the best imaging modality for the diagnosis of calvarial bone/bone marrow lesions. Usually, a combination of bone scintigraphy, CT, and MR is recommended for an imaging diagnosis, and if clinically needed, follow-up imaging is recommended (21). Recently, the use of 2-deoxy-2-[^{18}F] fluoro-D-glucose (^{18}FDG) PET or PET-CT have been used to detect bone marrow metastases (22, 23). ^{18}FDG PET directly visualizes increased glucose metabolism that occurs in tumor cells in the bone marrow. However, in one study, ^{18}FDG PET produced more false-negative findings for bone metastases than for nonosseous metastases because of the low ^{18}FDG uptake by bone (23). In addition, PET has lower spatial resolution than MRI and requires the intravenous injection of radioisotope, whereas MRI provides higher spatial resolution, better tissue contrast, and no radioisotope use. The present study demonstrates that the addition of DWI to routine brain MRI in patients with suspected metastases can aid in the diagnosis of cranial bone marrow metastases, in addition to the diagnosis of parenchymal metastases. The excellent lesion contrast obtained with DWI also implies that its use would enhance confidence rates for the diagnosis of cranial bone marrow metastases, especially by less experienced radiologists and trainees.

Several study limitations need consideration. First, we did not compare DWIs with fat-suppressed conventional MR images, and if fat-suppressed MR images had been used, the advantages of DWI may have been reduced. Second, although we used the SENSE technique to reduce susceptibility artifacts, not all image distortion was removed. In addition, routine brain echo-planar diffusion sequences for looking at the brain might be suboptimal for calvarial bone/bone marrow evaluations. Moreover, an optimized DWI technique recently has been developed for whole body malignancy screening (18). Third, we did not evaluate DWI in patients with anemia and/or a hematologic disorder. Anemia associated with red marrow reconversion alters bone/bone marrow DWI signals, and therefore affects lesion conspicuousness in patients with cranial bone/bone marrow metastases. Finally, the number of cases enrolled in the present study was small, and thus, we believe that a further investigation of these techniques in a larger series is necessary to verify results.

We conclude that DWI with SENSE can be used to aid in the detection of cranial bone/bone marrow metastases in

conjunction with conventional MR sequences.

References

1. Yildirim T, Agildere AM, Oguzkurt L, Barutcu O, Kizilkilic O, Kocak R, et al. MRI evaluation of cranial bone marrow signal intensity and thickness in chronic anemia. *Eur J Radiol* 2005;53:125-130
2. Loevner LA, Tobey JD, Yousem DM, Sonners AI, Hsu WC. MR imaging characteristics of cranial bone marrow in adult patients with underlying systemic disorders compared with healthy control subjects. *AJNR Am J Neuroradiol* 2002;23:248-254
3. Vogler JB 3rd, Murphy WA. Bone marrow imaging. *Radiology* 1988;168:679-693
4. Daffner RH, Lupetin AR, Dash N, Deeb ZL, Sefczek RJ, Schapiro RL. MRI in the detection of malignant infiltration of bone marrow. *AJR Am J Roentgenol* 1986;146:353-358
5. Nyman R, Rehn S, Glimelius B, Hagberg H, Hemmingsson A, Jung B, et al. Magnetic resonance imaging in diffuse malignant bone marrow disease. *Acta Radiol* 1987;28:199-205
6. Ricci C, Cova M, Kang YS, Yang A, Rahmouni A, Scott WW Jr et al. Normal age-related patterns of cellular and fatty bone marrow distribution in the axial skeleton: MR imaging study. *Radiology* 1990;177:83-88
7. Herneth AM, Friedrich K, Weidekamm C, Schibany N, Krestan C, Czerny C, et al. Diffusion weighted imaging of bone marrow pathologies. *Eur J Radiol* 2005;55:74-83
8. Raya JG, Dietrich O, Reiser MF, Baur-Melnyk A. Techniques for diffusion-weighted imaging of bone marrow. *Eur J Radiol* 2005;55:64-73
9. Baur A, Stabler A, Bruning R, Bartl R, Krodel A, Reiser M, et al. Diffusion-weighted MR imaging of bone marrow: differentiation of benign versus pathologic compression fractures. *Radiology* 1998;207:349-356
10. Castillo M, Arbelaez A, Smith JK, Fisher LL. Diffusion-weighted MR imaging offers no advantage over routine noncontrast MR imaging in the detection of vertebral metastases. *AJNR Am J Neuroradiol* 2000;21:948-953
11. Herneth AM, Philipp MO, Naude J, Funovics M, Beichel RR, Bammer R, et al. Vertebral metastases: assessment with apparent diffusion coefficient. *Radiology* 2002;225:889-894
12. Maeda M, Sakuma H, Maier SE, Takeda K. Quantitative assessment of diffusion abnormalities in benign and malignant vertebral compression fractures by line scan diffusion-weighted imaging. *AJR Am J Roentgenol* 2003;181:1203-1209
13. Zhou XJ, Leeds NE, McKinnon GC, Kumar AJ. Characterization of benign and metastatic vertebral compression fractures with quantitative diffusion MR imaging. *AJNR Am J Neuroradiol* 2002;23:165-170
14. Byun WM, Shin SO, Chang Y, Lee SJ, Finsterbusch J, Frahm J. Diffusion-weighted MR imaging of metastatic disease of the spine: assessment of response to therapy. *AJNR Am J Neuroradiol* 2002;23:906-912
15. Meyer JR, Gutierrez A, Mock B, Hebron D, Prager JM, Gorey MT, et al. High-b-value diffusion-weighted MR imaging of suspected brain infarction. *AJNR Am J Neuroradiol* 2000;21:1821-1829
16. Mirowitz SA, Apicella P, Reinus WR, Hammerman AM. MR imaging of bone marrow lesions: relative conspicuousness on T1-weighted, fat-suppressed T2-weighted, and STIR images. *AJR Am J Roentgenol* 1994;162:215-221
17. Stadnik TW, Chaskis C, Michotte A, Shabana WM, van Rompaey K, Luypaert R, et al. Diffusion-weighted MR imaging of intracerebral masses: comparison with conventional MR imaging and histologic findings. *AJNR Am J Neuroradiol* 2001;22:969-976
18. Takahara T, Imai Y, Tamashita T, Yasuda S, Nasu S, Van Cauteren M. Diffusion-weighted whole body imaging with background body signal suppression (DWIBS): technical improvement using free breathing, STIR and high resolution 3D display. *Radiat Med* 2004;22:275-282
19. Bammer R, Keeling SL, Augustin M, Pruessmann KP, Wolf R, Stollberger R, et al. Improved diffusion-weighted single-shot echo-planar imaging (EPI) in stroke using sensitivity encoding (SENSE). *Magn Reson Med* 2001;46:548-554
20. Chan JH, Peh WC, Tsui EY, Chau LF, Cheung KK, Chan KB, et al. Acute vertebral body compression fractures: discrimination between benign and malignant causes using apparent diffusion coefficients. *Br J Radiol* 2002;75:207-214
21. Haubold-Reuter BG, Duewell S, Schilcher BR, Marincek B, von Schulthess GK. The value of bone scintigraphy, bone marrow scintigraphy and fast spin-echo magnetic resonance imaging in staging of patients with malignant solid tumours: a prospective study. *Eur J Nucl Med* 1993;20:1063-1069
22. Daldrup-Link HE, Franzius C, Link TM, Laukamp D, Sciuk J, Jurgens H, et al. Whole-body MR imaging for detection of bone metastases in children and young adults: comparison with skeletal scintigraphy and FDG PET. *AJR Am J Roentgenol* 2001;177:229-236
23. Hamaoka T, Madewell JE, Podoloff DA, Hortobagyi GN, Ueno NT. Bone imaging in metastatic breast cancer. *J Clin Oncol* 2004;22:2942-2953